

Deriving a topology function to be used in the reaction diffusion equation for optimization of structures with thermal and mechanical boundary conditions

Ehsan Dehghanipour^a, Ali Ghoddosian^b

^aPh.D student, Faculty of Mechanical Engineering, Semnan University, Semnan, Iran.

^bAssociate Professor, Faculty of Mechanical engineering, Semnan University, Semnan, Iran.

(Communicated by Madjid Eshaghi Gordji)

Abstract

A topological derivative of the Lagrangian is required for optimization of structures with thermal and mechanical boundary conditions by the level-set method using the reaction diffusion equation. In this study, drawing on the relationship between the shape derivative and the topological derivative, the topological derivative of the Lagrangian was obtained by Reynolds' transport theorem. Given that introducing holes to the topology creates boundaries, the derivative was found by incorporating the boundary integral into the Reynolds' transport theorem and analyzing the stress over the hole boundaries. The temperature was assumed to be dependent on topology in the present study under thermal and mechanical boundary conditions. Placing a hole in the structure affects the temperature of the remaining elements. Penalty factor is enforced on thermal conductivity for removed elements, and the result is taken into consideration in the Laplace's equation expressing the steady-state conductive heat transfer.

Keywords: Topological Derivative, Shape Derivative, Reynolds' Transport Theorem, Reaction Diffusion Equation, Thermal and Mechanical Boundary Conditions.

*Corresponding author

Email addresses: e.dehghanipour@semnan.ac.ir (Ehsan Dehghanipour), aghoddosian@semnan.ac.ir (Ali Ghoddosian)

1. Introduction

Topology Optimization (TO) is a reliable tool for constructing highly-efficient structures with minimal use of materials. In this method of optimization, system components can be removed from or introduced to the domain. Although the optimization can be applied to both continuum and discrete structures, here, we focus on continuum TO.

The aim of TO in a continuum domain is to achieve the optimal distribution for a set amount of construction materials in a predefined domain while satisfying the system performance requirements and problem constraints. Researchers have proposed several TO methods for the continuum domain. One of the first, most prominent of these methods is the homogenization method, introduced in 1988 by Bendsoe [4]. In this scheme, first, a set of fine holes are introduced to the domain, and then, an optimization problem is solved to create an optimal distribution of the holes. Taking the TO approach to replace size optimization in homogenization allows for creating new holes in the domain. However, in some cases, the homogenization method provides a suboptimal solution, and the resulting structure can come with extremely-fine holes that undermine the practical value of the method [42]. In other words, this TO scheme results in a "gray" optimal structure. Accordingly, different methods have been proposed to improve the efficiency of homogenization, all of which are based on penalizing the gray parts of the structure. Introduced in 1989 by Bendsoe, Solid Isotropic Material with Penalization (SIMP) is a prominent example of such methods [5]. The method assumes homogeneous and isotropic materials. The algorithm begins with discretizing the domain to fixed-density elements. Further, the elasticity of each element is a function of its density ($E = p^P E^O$). Where P represents the density of the element, P is the penalty factor, and E denotes the elasticity of the materials.

Examples of other TO methods include the Evolutionary Structural Optimization (ESO). This scheme, introduced in 1997 by Xie et al., involves removing elements with the least effect on the field response [40, 41]. Similar to the previous method, the ESO begins by discretizing the design domain using suitable elements. Knowing the finite-element analysis will suffice for implementing this method as it features a simple, smart algorithm that involves removing elements with the least impact on the response. However, a notable drawback of this scheme is that it is prone to be trapped in local optima [41]. Others, including the bubble method [14] and reverse adaptivity [28], followed the discussed methods, with each offering their particular advantages and drawbacks. What is shared by all these methods is the optimization variable they consider. In fact, in all these methods, material properties are considered as optimization variables. For example, in the TO of a cantilever beam, after meshing, the thickness of each element will be taken as the optimization variable in all discussed methods.

In addition, the level-set method, as an efficient TO method, has been employed as an effective optimization method for continuum domains. The main difference between this and other methods lies in the optimization variable. The level-set method assumes interior and exterior boundaries as optimization variables with each boundary moving at a defined velocity in the appropriate direction that yields the optimal structure. In 1998, to show the structural boundary variations, Osher and Sethian introduced the Hamilton-Jacobi equation. The boundary assumed to be able to move at a set velocity to allow a solution for the Hamilton-Jacobi equation. The level-set method was first used for structural TO in 2000 [31]. In their proposed method, Wiegmann and Sethian moved the boundaries in proportion to the stress exerted on them. The boundaries, in this method, were defined as the zero iso-surface of the level-set function. By solving Hamilton-Jacobi equation, the level-set function changes forms, leading to zero iso-surface and domain boundaries assuming new positions. The definition of boundary velocity as stress is what links TO and the level-set method. Wiegmann

and Sethian showed if the boundaries move at a velocity equal to the stress over the boundary, the structure transforms into a configuration with minimum potential energy. Later Osher and Santosa employed the level-set method for structural frequency optimization [26]. In their work, the authors calculated the velocity and applied the geometrical constraints by the projected gradient method. Wang et al. [37] proposed the velocity vector based on the boundary form and changes in the sensitivity as a significant physical link between the shape derivative and the robust level-set method. The method was later expanded through color level-set methods [38] to represent TO and the shapes of multi-phase design domains. Allaire et al. [2] independently presented a similar level-set method to improve the shape and topology of the structure. In this method, the velocity vector is derived from the shape sensitivity analysis and the motion of the boundaries is a function of the solution of the Hamilton-Jacobi equation. Yamada et al. [43, 27] presented an advanced boundary representation method based on boundary expression methods. In this method, the level-set function is updated by the reaction diffusion equation based on a topological derivative of the objective function. The method allows new boundaries to form during optimization by topological variations without requiring a re-initialization of the level-set function-unlike the Hamilton-Jacobi equation. Another attraction of the reaction diffusion equation is that it can be used for optimizing complex geometries through a "regularization" parameter.

Further, several researchers worked on different methods which created holes in the topology. A standard method is to assume holes are present in the structure from the very beginning. In this method, selecting and controlling the number and size of the initial holes has proved challenging. The studies addressing this method include the work of Bendsoe et al. [4, 6, 7] proposing the homogenization method. Examples of level-set-based TO with initial holes include the works of Wang et al. [37, 36], and Xia and Wang [39] employed this method for thermo-elastic structures. Eschenauer et al. [14] and Schumacher [30] proposed another TO approach that was later expanded once the mathematical concept of topological derivative was introduced (examples include Sokolowski and Zochowski [32]; Cea et al. [9]; Garreau et al. [18]). The concept was further expanded by Burger et al. [8], Allaire et al. [1], Yulin and Xiaoming [46], A. A. Novotny [24, 25]. The present study used the topological derivative of the Lagrangian. Optimization is carried out by substituting it in the reaction diffusion equation.

Optimization of elastic structures in thermal environments, also known as thermo-elastic structures, has become a topic of interest in recent years. In such environments, the structure experiences damage due to thermal stresses. Traditionally, these stresses were diminished or eliminated by allowing the structure to expand in some or all directions. Examples of such a design method include expansion joints in concrete structures and gas turbine components. This solution, however, is not applicable to all structures, an example being the nozzle of an airplane. Exhaust gases temperature from the nozzle causes serious damage to the nozzle, engine, and fuselage of the airplane. Optimization techniques are rendered necessary by the impracticality of using the expansion method to prevent the nozzle structure from developing thermal stresses. As one of the most advanced of design techniques, topology optimization is an ideal option. Various methods of topology optimization for thermo-elastic structures are introduced in what follows.

Using the homogenization method, a study due to Rodrigues et al. [29] considered topology optimization of thermo-elastic structures where they combined homogenization on periodic microstructures with finite element formulations. This resulted in reduced thermal strains in the final structure. In [20], the solid isotropic material with penalization (SIMP) method was used for topology optimization of thermo-elastic structures to minimize the strain energy, and the sensitivity analysis were carried out based on the adjoint method. In [44], the buckling of a thermo-elastic structure under time dependent loading was analyzed using the SIMP method. In [45], frequency responses of a

thermo-elastic structure were minimized through the SIMP method. Another study [21] combined the SIMP and guide weight methods to minimize the compliance function for a thermo-elastic structure. In study [47] used the SIMP method to make a comparison between the minimization of strain energy and compliance for thermo-elastic structures. As another topology optimization technique, the rational approximation of material properties (RAMP) differs from the SIMP method in that the zero density material distribution function of the SIMP method for thermo-elastic problems is always a challenge [33, 17], which is resolved by RAMP [33]. The superior performance of RAMP is demonstrated in [17]. This technique was used for the optimization of thermo-elastic structures, for instance by [12], which proposed the stress-relaxation method for stress constraints. Another efficient method for the topology optimization of thermo-elastic structures is the level-set (LS) approach [19, 11], where design variables are the boundaries of the structure. The study by Xia [39] is among the most important studies adopting this approach. In this study, the compliance function was minimized for a thermo-elastic structure. The effects of material properties for multi phase thermo-elastic structures were presented through the LS approach in [34]. A comparison was made in [22] between minimizing strain energy, compliance and stress in thermo-elastic structures through the LS approach. In [13], topological sensitivity for stress constraints was analyzed using the LS approach in a thermo-elastic structure.

All the above studies on the topology optimization of thermo-elastic structures through homogenization, SIMP, RAMP, and LS methods were similar in that they considered the temperature of each element to be constant during the course of optimization. In other words, temperature was considered to be independent of the topological changes. In fact, in deriving sensitivity functions when holes were created under mechanical and thermal loads, temperature variations were not taken into account. In the study by Xia [39], for instance, no topology dependent temperature variations were observed in the velocity term of the Hamilton- Jacobi equation, something which points to the novelty of the present work. Indicating the temperature that depends on topological changes, a topology function was derived in the present study through relevant mathematical methods.

2. Defining the Optimization Problem

According to Fig. 1, the structural boundary is defined as follows

$$\partial\Omega = \Gamma_u \cup \Gamma_T \cup \Gamma_H \cup \Gamma_M \cup \Gamma_F \quad (1)$$

The Displacement boundary is denoted by Γ_u , temperature boundary by Γ_T , thermal load boundary by Γ_H , mechanical load boundary by Γ_M , and the free structural boundary by Γ_F .

The problem is governed by the equilibrium equation stated as follows:

$$\begin{cases} -\nabla \cdot \sigma(\mathbf{u}) = 0 & \text{in } \Omega \\ \mathbf{u} = \mathbf{0} & \text{on } \Gamma_u \\ \mathbf{F} = \mathbf{F}_m & \text{on } \Gamma_M \end{cases} \quad (2)$$

Heat transfer analysis is necessary under temperature and thermal boundary conditions. The below equation can be established assuming heat transfer by conduction:

$$\begin{cases} -\nabla \cdot (\mathbf{K}\nabla T) = 0 & \text{in } \Omega \\ T = T_0 & \text{on } \Gamma_T \\ \mathbf{K}\nabla T \cdot \mathbf{n} = q & \text{in } \Gamma_H \\ \mathbf{K}\nabla T \cdot \mathbf{n} = 0 & \text{in } \Gamma_F \end{cases} \quad (3)$$

Where

$$\mathbf{K} = k\mathbf{I} \quad (4)$$

Where k represents thermal conductivity coefficient, q is heat flux over the boundary, and \mathbf{n} is the normal vector on the boundary.

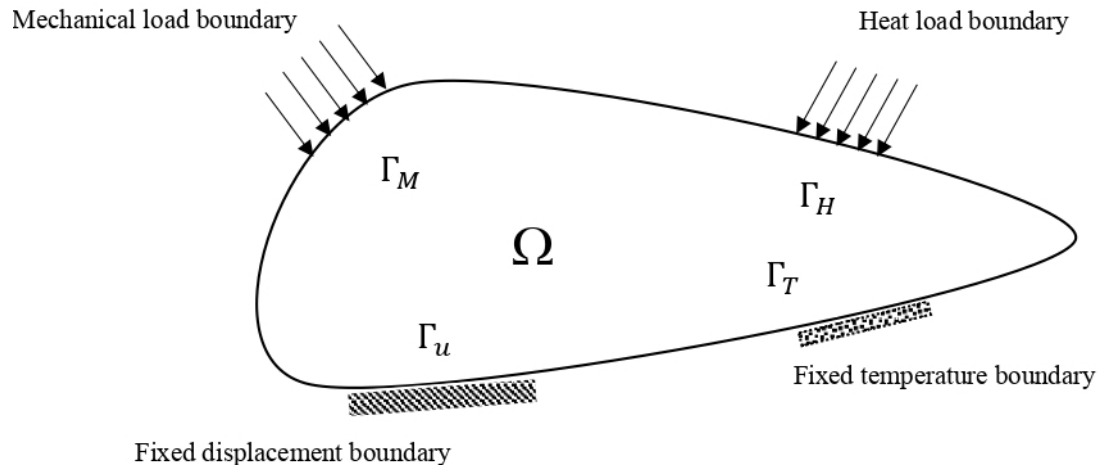


Fig. 1. The structural boundaries.

The two equations above are coupled with the stress-strain relation:

$$\sigma = \mathbf{C}(\varepsilon(\mathbf{u}) - \varepsilon_{th}(T)) \quad (5)$$

The mechanical strain is defined as follow

$$\varepsilon(\mathbf{u}) = \frac{1}{2}(\nabla\mathbf{u} + (\nabla\mathbf{u})^T) \quad (6)$$

The thermal strain is defined as follow

$$\varepsilon_{th}(T) = \alpha T\Phi^T, \quad \Phi = [1 \ 1 \ 0] \quad (7)$$

\mathbf{C} represents the elastic coefficient tensor and α , in thermal strain, is the thermal expansion coefficient. The integral form of the equilibrium equation (2) is as follows

$$a(\mathbf{u}, \mathbf{v}) = \gamma(T, \mathbf{v}) + l_f(\mathbf{v}), \quad \mathbf{u} \in Z(\Omega), \quad \forall v \in Z(\Omega) \quad (8)$$

Where

$$a(\mathbf{u}, \mathbf{v}) = \int_{\Omega} \mathbf{C}\varepsilon(\mathbf{u})\varepsilon(\mathbf{v})d\Omega \quad (9)$$

$$l_f(\mathbf{v}) = \int_{\Gamma_M} \mathbf{F}_m \mathbf{v} d\Gamma \quad (10)$$

$$\gamma(T, \mathbf{v}) = \int_{\Omega} \mathbf{C}\varepsilon_{th}(T)\varepsilon(\mathbf{v})d\Omega \quad (11)$$

$$Z(\Omega) = \{\mathbf{v} \in H^1(\Omega)^N \mid \mathbf{v} = 0 \text{ on } \Gamma_D\} \quad (12)$$

Where $Z(\Omega)$ is the allowable space for the displacement vector. The integral form of the thermal conduction equation is as follows

$$\mathbf{b}(\mathbf{T}, \bar{\mathbf{T}}) = l_h(\bar{\mathbf{T}}) \quad (13)$$

$$\mathbf{b}(\mathbf{T}, \bar{\mathbf{T}}) = \int_{\Omega} k \nabla T \cdot \nabla \bar{\mathbf{T}} \quad (14)$$

$$l_h(\bar{\mathbf{T}}) = \int_{\Gamma_h} q \bar{\mathbf{T}} d\Gamma \quad (15)$$

$$Y = \{ \bar{\mathbf{T}} \in H^1(\Omega)^N \mid \bar{\mathbf{T}} = \mathbf{T}_0 \text{ on } \Gamma_{T_0} \} \quad (16)$$

Where Y is the allowable space for the temperature field. Under thermal and mechanical boundary conditions, the objective function in the optimization problem, referred to as "compliance", is defined as follows

$$J = \gamma(T, \mathbf{u}) + l_f(\mathbf{u}) \quad (17)$$

Where

$$l_f(\mathbf{u}) = \int_{\Gamma_M} \mathbf{F}_m \mathbf{u} d\Gamma \quad (18)$$

$$\gamma(T, \mathbf{u}) = \int_{\Omega} \mathbf{C} \varepsilon_{th}(T) \varepsilon(\mathbf{u}) d\Omega \quad (19)$$

A constraint stating that the material volume \mathbf{V} should not exceed a given upper bound $\bar{\mathbf{V}}$ is given by

$$\mathbf{V} = \int_{\Omega} dx \leq \bar{\mathbf{V}} \quad (20)$$

A structure is represented as an open-bounded set $\Omega \subset \mathbb{R}^d$ ($d = 2$ or 3). It is necessary that, during optimization, all admissible structures remain within a fixed reference domain $D \subset \mathbb{R}^d$ that is, $\Omega \subset D$. The set of admissible shapes can be defined

$$U_{ad} = \{ \Omega \subset D, \mathbf{V} \leq \bar{\mathbf{V}} \} \quad (21)$$

Defining the optimization problem:

$$\inf_{\Omega \in U_{ad}} J \quad (22)$$

3. Optimization Method

The reaction diffusion equation is used in the level-set-based optimization:

$$\frac{\partial \varphi}{\partial t} = D_T L + \tau \nabla^2 \varphi \quad (23)$$

In the reaction diffusion equation, φ represents the level-set function, which is defined as follows:

$$\begin{cases} \varphi(x) = 0 & \forall x \in \partial\Omega \\ \varphi(x) > 0 & \forall x \in \Omega \setminus \partial\Omega \\ \varphi(x) < 0 & \forall x \in D \setminus \partial\Omega \end{cases} \quad (24)$$

In the established equation, $\varphi(x) = 0$ shows the structural boundary, $\varphi(x) > 0$ is the material phase and $\varphi(x) < 0$ is the void.

In the reaction diffusion equation, $D_T L$ denotes the topological derivative of the Lagrangian function and τ is the regularization parameter corresponding to the second-degree gradient of the level-set function. What is important is that the topological derivative of the Lagrangian is found. By forming the Lagrangian function, we have:

$$L = J + \gamma(T, \mathbf{w}) + l_f(\mathbf{w}) - a(\mathbf{u}, \mathbf{w}) + \lambda(V - \bar{V}) \tag{25}$$

where \mathbf{w} and λ are the Lagrange multipliers.

λ is updated during the optimization according to the augmented lagrange multiplier method [23] as

$$\lambda^{m+1} = \max\{0, \lambda^m + \frac{1}{\beta}(V^m - \bar{V})\} \tag{26}$$

Where $\beta > 0$ is a penalty parameter.

By substituting in Lagrange's equation, we have:

$$\begin{aligned} L = & \int_{\Omega} \mathbf{C}\varepsilon_{th}(T)\varepsilon(\mathbf{u})d\Omega + \int_{\Gamma_M} \mathbf{F}_m \mathbf{u} d\Gamma - \int_{\Omega} \mathbf{C}\varepsilon(\mathbf{u})\varepsilon(\mathbf{w})d\Omega \\ & + \int_{\Omega} \mathbf{C}\varepsilon_{th}(T)\varepsilon(\mathbf{w})d\Omega + \int_{\Gamma_M} \mathbf{F}_m \mathbf{w} d\Gamma + \lambda(V - V_{max}) \end{aligned} \tag{27}$$

By rearranging the equation above, we have:

$$\begin{aligned} L = & \int_{\Omega} \mathbf{C}\varepsilon_{th}(T)[\varepsilon(\mathbf{u}) + \varepsilon(\mathbf{w})]d\Omega + \int_{\Gamma_M} \mathbf{F}_m (\mathbf{u} + \mathbf{w}) d\Gamma \\ & - \int_{\Omega} \mathbf{C}\varepsilon(\mathbf{u})\varepsilon(\mathbf{w})d\Omega + \lambda(V - \bar{V}) \end{aligned} \tag{28}$$

The material derivative of the Lagrangian is used for this purpose [10, 12, 35]. The aim is to find the adjoint equation, which will be used to find the multiplier \mathbf{w} . The material derivative of Lagrange's equation is as follows

$$L' = J' + \gamma'(T, \mathbf{w}) + l'_f(\mathbf{w}) - a'(\mathbf{u}, \mathbf{w}) + \lambda V' \tag{29}$$

The material derivative of the objective function

$$\begin{aligned} J' = & \gamma(T, \mathbf{u}') + \gamma(T', \mathbf{u}) + l_f(\mathbf{u}') + \int_{\partial\Omega} \mathbf{C}\varepsilon_{th}(T)\varepsilon(\mathbf{u})\mathbf{V} \cdot \mathbf{n} d\Gamma \\ & + \int_{\Gamma_M} (\nabla(\mathbf{F}_m \mathbf{u}) \cdot \mathbf{n} + \kappa \mathbf{F}_m \mathbf{u})\mathbf{V} \cdot \mathbf{n} d\Gamma \end{aligned} \tag{30}$$

Where

$$\kappa = \text{div } \mathbf{n} \tag{31}$$

The material derivative of other terms of Lagrange's equation

$$a'(\mathbf{u}, \mathbf{w}) = a(\mathbf{u}', \mathbf{w}) + a(\mathbf{u}, \mathbf{w}') + \int_{\partial\Omega} \mathbf{C}\varepsilon(\mathbf{u})\varepsilon(\mathbf{w})\mathbf{V} \cdot \mathbf{n} d\Gamma \tag{32}$$

$$\gamma'(T, \mathbf{w}) = \gamma(T, \mathbf{w}') + \gamma(T', \mathbf{w}) + \int_{\partial\Omega} \mathbf{C}\varepsilon_{th}(T)\varepsilon(\mathbf{w})\mathbf{V} \cdot \mathbf{n} d\Gamma \tag{33}$$

$$l'_f(\mathbf{w}) = l_f(\mathbf{w}') + \int_{\Gamma_M} (\nabla(\mathbf{F}_m \mathbf{w}) \cdot \mathbf{n} + \kappa \mathbf{F}_m \mathbf{w})\mathbf{V} \cdot \mathbf{n} d\Gamma \tag{34}$$

$$V' = \int_{\partial\Omega} \mathbf{V} \cdot \mathbf{n} d\Gamma \tag{35}$$

By substituting in the material derivative of the Lagrangian, we have:

$$\begin{aligned}
 L' = & \gamma(T, \mathbf{u}') + \gamma(T', \mathbf{u}) + l_f(\mathbf{u}') + \int_{\partial\Omega} \mathbf{C}\varepsilon_{th}(T)\varepsilon(\mathbf{u})\mathbf{V} \cdot \mathbf{n}d\Gamma \\
 & + \int_{\Gamma_F} (\nabla(\mathbf{F}_m\mathbf{u}) \cdot \mathbf{n} + \kappa\mathbf{F}_m\mathbf{u})\mathbf{V} \cdot \mathbf{n}d\Gamma + \gamma(T, \mathbf{w}') + \gamma(T', \mathbf{w}) \\
 & + \int_{\partial\Omega} \mathbf{C}\varepsilon_{th}(T)\varepsilon(\mathbf{w})\mathbf{V} \cdot \mathbf{n}d\Gamma + l_f(\mathbf{w}') \\
 & + \int_{\Gamma_F} (\nabla(\mathbf{F}_m\mathbf{w}) \cdot \mathbf{n} + \kappa\mathbf{F}_m\mathbf{w})\mathbf{V} \cdot \mathbf{n}d\Gamma - a(\mathbf{u}, \mathbf{w}') - a(\mathbf{u}', \mathbf{w}) \\
 & - \int_{\partial\Omega} \mathbf{C}\varepsilon(\mathbf{u})\varepsilon(\mathbf{w})\mathbf{V} \cdot \mathbf{n}d\Gamma + \lambda \int_{\partial\Omega} V \cdot \mathbf{n}d\Gamma
 \end{aligned} \tag{36}$$

By taking into account the terms containing \mathbf{w}' , summing them up, and equating to zero, the equilibrium equation is obtained.

$$a(\mathbf{u}, \mathbf{w}') = \gamma(T, \mathbf{w}') + l_f(\mathbf{w}') \tag{37}$$

By taking into account the terms containing \mathbf{u}' , summing them up, and equating to zero, the adjoint equation is obtained.

$$a(\mathbf{u}, \mathbf{u}') = a(\mathbf{u}', \mathbf{w}) \tag{38}$$

Based on the definition of $a(\mathbf{u}, \mathbf{u}')$ and $a(\mathbf{u}', \mathbf{w})$ in Eq. (9), it is concluded from the adjoint equation that:

$$\mathbf{u} = \mathbf{w} \tag{39}$$

4. Topological derivative

Therefore, the topological derivative of the Lagrangian can be obtained. Thus, finding the topological derivative according to Novotny’s theory [16, 25]. According to Fig. 2, in this method, the topological derivative is stated as follows

$$D_T = \lim_{\varepsilon \rightarrow 0} \frac{\psi(\Omega_\varepsilon) - \psi(\Omega)}{f(\varepsilon)} \tag{40}$$

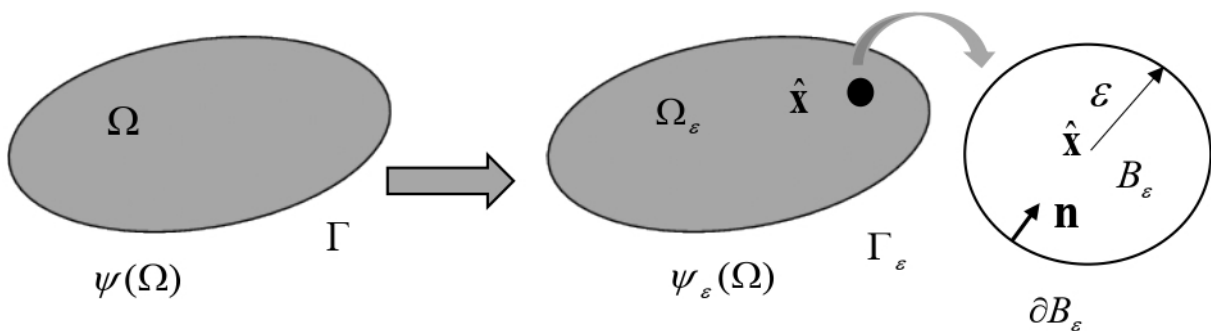


Fig. 2. Topological changes due to the introduction of a new hole.

Based on the theory, the relationship between the shape and topological derivatives is defined as:

$$D_T = \lim_{\varepsilon \rightarrow 0} \frac{1}{f'(\varepsilon)} \frac{d}{d\tau} \psi(\Omega_\tau) \Big|_{\tau=0} \tag{41}$$

Where

$$\Omega_\tau := \left\{ \mathbf{x}_\tau \in \mathbb{R}^2 : \mathbf{x} \in \Omega_\varepsilon, \mathbf{x}_\tau = \mathbf{x} + \tau \mathbf{v}, \mathbf{x}_\tau \Big|_{\tau=0} = \mathbf{x}, \Omega_\tau \Big|_{\tau=0} = \Omega_\varepsilon \right\} \quad (42)$$

The velocity vector \mathbf{v} is defined as follows

$$\begin{cases} \mathbf{v} = -\mathbf{n} & \text{on } \partial B_\varepsilon \\ \mathbf{v} = 0 & \text{on } \partial \Omega \end{cases} \quad (43)$$

Thermal conductivity coefficient and Young's modulus are defined as follows considering the topology conditions:

$$K = \begin{cases} K & \text{on } \Omega \setminus \bar{B}_\varepsilon \\ P_T K & \text{on } B_\varepsilon \end{cases} \quad (44)$$

$$E = \begin{cases} E & \text{on } \Omega \setminus \bar{B}_\varepsilon \\ P_M E & \text{on } B_\varepsilon \end{cases} \quad (45)$$

where P_M and P_T are penalty factors.

The theory can be applied to find the derivative of the Lagrangian. It will suffice that

$$\psi(\Omega_\tau) = L \quad (46)$$

Where

$$L = 2 \int_\Omega \mathbf{C} \varepsilon_{th}(T) \varepsilon(\mathbf{u}) d\Omega + 2 \int_{\Gamma_M} \mathbf{F}_m \mathbf{u} d\Gamma - \int_\Omega \mathbf{C} \varepsilon(\mathbf{u}) \varepsilon(\mathbf{u}) d\Omega + \lambda(V - \bar{V}) \quad (47)$$

Therefore, based on Eq. (41):

$$D_T L = \lim_{\varepsilon \rightarrow 0} \frac{1}{f'(\varepsilon)} \frac{d}{d\tau} L \Big|_{\tau=0} \quad (48)$$

Where

$$\begin{aligned} \frac{d}{d\tau} L \Big|_{\tau=0} &= \frac{d}{d\tau} \left(2 \int_\Omega \mathbf{C} \varepsilon_{th}(T) \varepsilon(\mathbf{u}) d\Omega \right) \Big|_{\tau=0} + \frac{d}{d\tau} \left(2 \int_{\Gamma_M} \mathbf{F}_m \mathbf{u} d\Gamma \right) \Big|_{\tau=0} \\ &+ \frac{d}{d\tau} \left(- \int_\Omega \mathbf{C} \varepsilon(\mathbf{u}) \varepsilon(\mathbf{u}) d\Omega \right) \Big|_{\tau=0} + \frac{d}{d\tau} \left(\lambda(V - \bar{V}) \right) \Big|_{\tau=0} \end{aligned} \quad (49)$$

The terms on the right side of the above equation, the shape derivatives, are defined by the Reynolds' transport theorem:

$$\begin{aligned} \frac{d}{d\tau} \left(2 \int_\Omega \mathbf{C} \varepsilon_{th}(T) \varepsilon(\mathbf{u}) d\Omega \right) \Big|_{\tau=0} &= 2 \int_{\Omega_\varepsilon} \frac{\partial}{\partial \tau} (\mathbf{C} \varepsilon_{th}(T_\tau) \varepsilon(\mathbf{u}_\tau)) \Big|_{\tau=0} d\Omega_\varepsilon \\ &+ 2 \int_{\partial \Omega_\varepsilon} \mathbf{C} \varepsilon_{th}(T_\varepsilon) \varepsilon(\mathbf{u}_\varepsilon) (\mathbf{v} \cdot \mathbf{n}) d\Gamma \end{aligned} \quad (50)$$

$$\frac{d}{d\tau} \left(2 \int_{\Gamma_M} \mathbf{F}_m \mathbf{u} d\Gamma \right) \Big|_{\tau=0} = 2 \int_{\Gamma_M} \mathbf{F}_m \dot{\mathbf{u}} d\Gamma \quad (51)$$

$$\begin{aligned} \frac{d}{d\tau} \left(- \int_\Omega \mathbf{C} \varepsilon(\mathbf{u}) \varepsilon(\mathbf{u}) d\Omega \right) \Big|_{\tau=0} &= - \int_{\Omega_\varepsilon} \frac{\partial}{\partial \tau} (\mathbf{C} \varepsilon(\mathbf{u}_\tau) \varepsilon(\mathbf{u}_\tau)) \Big|_{\tau=0} d\Omega_\varepsilon \\ &- \int_{\partial \Omega_\varepsilon} \mathbf{C} \varepsilon(\mathbf{u}_\varepsilon) \varepsilon(\mathbf{u}_\varepsilon) (\mathbf{v} \cdot \mathbf{n}) d\Gamma \end{aligned} \quad (52)$$

$$\frac{d}{d\tau} \left(\lambda(V - \bar{V}) \right) \Big|_{\tau=0} = \lambda \int_{\partial \Omega_\varepsilon} \mathbf{v} \cdot \mathbf{n} d\Gamma \quad (53)$$

Based on Eqs.9 and 11, the first terms of Eqs.50 and 52:

$$2 \int_{\Omega_\varepsilon} \frac{\partial}{\partial \tau} (\mathbf{C}\varepsilon_{th}(T_\tau)\varepsilon(\mathbf{u}_\tau)) \Big|_{\tau=0} d\Omega_\varepsilon = 2\gamma(T', \mathbf{u}) + 2\gamma(T, \mathbf{u}') \tag{54}$$

$$- \int_{\Omega_\varepsilon} \frac{\partial}{\partial \tau} (\mathbf{C}\varepsilon(\mathbf{u}_\tau)\varepsilon(\mathbf{u}_\tau)) \Big|_{\tau=0} d\Omega_\varepsilon = -a(\mathbf{u}, \mathbf{u}') - a(\mathbf{u}', \mathbf{u}) = -2a(\mathbf{u}, \mathbf{u}') \tag{55}$$

Then

$$\begin{aligned} \frac{d}{d\tau} L \Big|_{\tau=0} &= 2\gamma(T', \mathbf{u}) + 2\gamma(T, \mathbf{u}') + 2 \int_{\partial\Omega_\varepsilon} \mathbf{C}\varepsilon_{th}(T_\varepsilon)\varepsilon(\mathbf{u}_\varepsilon)(\mathbf{v} \cdot \mathbf{n})d\Gamma \\ &+ 2 \int_{\Gamma_M} \mathbf{F}_m \dot{\mathbf{u}}d\Gamma - 2a(\mathbf{u}, \mathbf{u}') - \int_{\partial\Omega_\varepsilon} \mathbf{C}\varepsilon(\mathbf{u}_\varepsilon)\varepsilon(\mathbf{u}_\varepsilon)(\mathbf{v} \cdot \mathbf{n})d\Gamma + \lambda \int_{\partial\Omega_\varepsilon} \mathbf{v} \cdot \mathbf{n}d\Gamma \end{aligned} \tag{56}$$

Considering that:

$$\dot{\mathbf{u}} = \frac{d}{d\tau} \mathbf{u} + \frac{d\mathbf{u}}{d\mathbf{x}} \frac{d\mathbf{x}}{d\tau} = \mathbf{u}' + (\nabla\mathbf{u})\mathbf{v} \tag{57}$$

Then, the fourth term of the Eq. (56):

$$2 \int_{\Gamma_M} \mathbf{F}_m \dot{\mathbf{u}}d\Gamma = 2l_f(\mathbf{u}') + 2 \int_{\Gamma_M} \mathbf{F}_m(\nabla\mathbf{u})\mathbf{v}d\Gamma \tag{58}$$

According to the equilibrium equation (Eq. 8):

$$2a(\mathbf{u}, \mathbf{u}') = 2\gamma(T, \mathbf{u}') + 2 l_f(\mathbf{u}') \tag{59}$$

Therefore:

$$\begin{aligned} \frac{d}{d\tau} L \Big|_{\tau=0} &= 2\gamma(T', \mathbf{u}) + 2 \int_{\partial\Omega_\varepsilon} \mathbf{C}\varepsilon_{th}(T_\varepsilon)\varepsilon(\mathbf{u}_\varepsilon)(\mathbf{v} \cdot \mathbf{n})d\Gamma + 2 \int_{\Gamma_M} \mathbf{F}_m(\nabla\mathbf{u})\mathbf{v}d\Gamma \\ &- \int_{\partial\Omega_\varepsilon} \mathbf{C}\varepsilon(\mathbf{u}_\varepsilon)\varepsilon(\mathbf{u}_\varepsilon)(\mathbf{v} \cdot \mathbf{n})d\Gamma + \lambda \int_{\partial\Omega_\varepsilon} \mathbf{v} \cdot \mathbf{n}d\Gamma \end{aligned} \tag{60}$$

The first term of the above equation can be rewritten based on stress as follow

$$2\gamma(T', \mathbf{u}) = 2 \int_{\Omega} \mathbf{C}\varepsilon_{th}(T')\varepsilon(\mathbf{u})d\Omega = 2 \int_{\Omega} \left[\sigma^T \varepsilon_{th}(T') + (\mathbf{C}\varepsilon_{th}(T))^T \varepsilon_{th}(T') \right] d\Omega \tag{61}$$

Under plane stress conditions:

$$(\mathbf{C}\varepsilon_{th}(T))^T \varepsilon_{th}(T') = \frac{2E\alpha^2 TT'}{1 - \nu} \tag{62}$$

Therefore:

$$2\gamma(T', \mathbf{u}) = 2(\alpha T' tr(\sigma) + \frac{2E\alpha^2 TT'}{1 - \nu}) \tag{63}$$

Let us now discuss T' from the above equation. For this purpose, the finite element form of Eq. (13) is used.

$$\mathbf{KT} = \mathbf{F} \Rightarrow \mathbf{K}'\mathbf{T} + \mathbf{KT}' = \mathbf{F}' \Rightarrow \mathbf{T}' = \mathbf{K}^{-1}(\mathbf{F}' - \mathbf{K}'\mathbf{T}) \tag{64}$$

With no thermal loads on the boundary:

$$\mathbf{T}' = -\mathbf{K}^{-1}\mathbf{K}'\mathbf{T} \tag{65}$$

Where

$$\mathbf{K}' = \begin{cases} 0 & \text{on } \Omega \setminus \bar{B}_\varepsilon \\ -(1 - P_T)\mathbf{K} & \text{on } B_\varepsilon \end{cases} \quad (66)$$

Therefore, four-node elements, the temperature of each element is determined as follows:

$$T' = \frac{1}{4} \sum_{i=1}^4 T'(i, 1) \quad (67)$$

Now, the second term of Eq. 60 is addressed.

$$2 \int_{\partial\Omega_\varepsilon} \mathbf{C}\varepsilon_{th}(T_\varepsilon)\varepsilon(\mathbf{u}_\varepsilon)(\mathbf{v} \cdot \mathbf{n})d\Gamma = 2 \int_{\partial\Omega} \mathbf{C}\varepsilon_{th}(T_\varepsilon)\varepsilon(\mathbf{u}_\varepsilon)(\mathbf{v} \cdot \mathbf{n})d\Gamma + 2 \int_{\partial B_\varepsilon} \mathbf{C}\varepsilon_{th}(T_\varepsilon)\varepsilon(\mathbf{u}_\varepsilon)(\mathbf{v} \cdot \mathbf{n})d\Gamma \quad (68)$$

Based on the relationship for velocity over the boundary in Eq. (43), the first term on the right of the equation is zero while the second term is as follows:

$$2 \int_{\partial B_\varepsilon} \mathbf{C}\varepsilon_{th}(T_\varepsilon)\varepsilon(\mathbf{u}_\varepsilon)(\mathbf{v} \cdot \mathbf{n})d\Gamma = -2 \int_{\partial B_\varepsilon} \mathbf{C}\varepsilon_{th}(T_\varepsilon)\varepsilon(\mathbf{u}_\varepsilon)(\mathbf{n} \cdot \mathbf{n})d\Gamma = -2 \int_{\partial B_\varepsilon} \mathbf{C}\varepsilon_{th}(T_\varepsilon)\varepsilon(\mathbf{u}_\varepsilon)d\Gamma \quad (69)$$

Therefore, stress analysis over hole boundary is necessary, and the above equation must be rewritten based on stress. Based on Eq. (5), and by substituting in the integral (69), we have:

$$\begin{aligned} -2 \int_{\partial B_\varepsilon} \mathbf{C}\varepsilon_{th}(T_\varepsilon)\varepsilon(\mathbf{u}_\varepsilon)d\Gamma &= -2 \int_{\partial B_\varepsilon} \varepsilon_{th}(T_\varepsilon)[\sigma + \mathbf{C}\varepsilon_{th}]d\Gamma \\ &= -2 \int_{\partial B_\varepsilon} \left[\sigma^T \varepsilon_{th}(T_\varepsilon) + (\mathbf{C}\varepsilon_{th}(T_\varepsilon))^T \varepsilon_{th}(T_\varepsilon) \right] d\Gamma \end{aligned} \quad (70)$$

Stress tensor over the hole boundary is defined as follows

$$\sigma(\mathbf{u}_\varepsilon)|_{\partial B_\varepsilon} = \sigma_\varepsilon^{nn}(\mathbf{n} \otimes \mathbf{n}) + \sigma_\varepsilon^{tn}(\mathbf{t} \otimes \mathbf{n}) + \sigma_\varepsilon^{nt}(\mathbf{n} \otimes \mathbf{t}) + \sigma_\varepsilon^{tt}(\mathbf{t} \otimes \mathbf{t}) \quad (71)$$

Based on boundary conditions over the hole,

$$\sigma(\mathbf{u}_\varepsilon)\mathbf{n} = \sigma_\varepsilon^{nn}\mathbf{n} + \sigma_\varepsilon^{tn}\mathbf{t} = 0 \Rightarrow \sigma_\varepsilon^{nn} = \sigma_\varepsilon^{tn} = 0 \text{ on } \partial B_\varepsilon \quad (72)$$

Therefore, the boundary integral is:

$$-2 \int_{\partial B_\varepsilon} \left[\sigma^T \varepsilon_{th}(T_\varepsilon) + (\mathbf{C}\varepsilon_{th}(T_\varepsilon))^T \varepsilon_{th}(T_\varepsilon) \right] d\Gamma = -2 \int_{\partial B_\varepsilon} \left[\sigma^{tt}\alpha T + (\mathbf{C}\varepsilon_{th}(T_\varepsilon))^T \varepsilon_{th}(T_\varepsilon) \right] d\Gamma \quad (73)$$

Tangential stress over the hole boundary is rewritten based on the principal stresses in polar coordinates:

$$\sigma_\varepsilon^{tt} = \frac{\sigma_1 + \sigma_2}{2} \left(1 + \frac{\varepsilon^2}{r^2}\right) - \frac{\sigma_1 - \sigma_2}{2} \left(1 + \frac{3\varepsilon^4}{r^4}\right) \cos 2\gamma + O(\varepsilon^{1-\mu}) \quad (74)$$

The principal stresses are defined as follows:

$$\begin{aligned} \sigma_{1,2} &= \frac{1}{2} [tr(\sigma) \pm \sqrt{(2\sigma^D \cdot \sigma^D)}] \\ \sigma^D &= \sigma - \frac{1}{2} tr(\sigma) \mathbf{I} \end{aligned} \quad (75)$$

Tangential stress over the hole boundary is created at $r = \varepsilon$:

$$\sigma_\varepsilon^{tt} = \sigma_1 + \sigma_2 - 2(\sigma_1 - \sigma_2) \cos 2\gamma \quad (76)$$

By substituting tangential stress in boundary integral (73):

$$\begin{aligned} & -2 \int_{\partial B_\varepsilon} \left[\sigma^{tt} \alpha T + (\mathbf{C} \varepsilon_{th}(T_\varepsilon))^T \varepsilon_{th}(T_\varepsilon) \right] d\Gamma = \\ & -2 \int_{\partial B_\varepsilon} \left[[\sigma_1 + \sigma_2 - 2(\sigma_1 - \sigma_2) \cos 2\gamma] \alpha T + (\mathbf{C} \varepsilon_{th}(T_\varepsilon))^T \varepsilon_{th}(T_\varepsilon) \right] d\Gamma \end{aligned} \quad (77)$$

By integration over the hole boundary:

$$\begin{aligned} & -2 \int_0^{2\pi} \left[[\sigma_1 + \sigma_2 - 2(\sigma_1 - \sigma_2) \cos 2\gamma] \alpha T + (\mathbf{C} \varepsilon_{th}(T_\varepsilon))^T \varepsilon_{th}(T_\varepsilon) \right] \varepsilon d\gamma \\ & = -2\varepsilon \left(\alpha T [(\sigma_1 + \sigma_2)\gamma - (\sigma_1 - \sigma_2) \sin 2\gamma] \Big|_0^{2\pi} + (\mathbf{C} \varepsilon_{th}(T_\varepsilon))^T \varepsilon_{th}(T_\varepsilon) \gamma \Big|_0^{2\pi} \right) \\ & = -4\pi\varepsilon \left[\alpha T \text{tr}(\sigma) + (\mathbf{C} \varepsilon_{th}(T_\varepsilon))^T \varepsilon_{th}(T_\varepsilon) \right] \end{aligned} \quad (78)$$

Under plane stress conditions:

$$-2 \int_{\partial B_\varepsilon} \left[\sigma^{tt} \alpha T + (\mathbf{C} \varepsilon_{th}(T_\varepsilon))^T \varepsilon_{th}(T_\varepsilon) \right] d\Gamma = -4\pi\varepsilon \left[\alpha T \text{tr}(\sigma) + \frac{2E\alpha^2 T^2}{1-\nu} \right] \quad (79)$$

The third term of Eq. 60: Based on the relationship for velocity over the boundary in Eq. (43),

$$2 \int_{\Gamma_M} \mathbf{F}_m(\nabla \mathbf{u}) \mathbf{v} d\Gamma = 0 \quad (80)$$

The fourth term of Eq. 60:

$$\begin{aligned} - \int_{\partial \Omega_\varepsilon} \mathbf{C} \varepsilon(\mathbf{u}_\varepsilon) \varepsilon(\mathbf{u}_\varepsilon) (\mathbf{v} \cdot \mathbf{n}) d\Gamma & = - \int_{\partial \Omega} \mathbf{C} \varepsilon(\mathbf{u}_\varepsilon) \varepsilon(\mathbf{u}_\varepsilon) (\mathbf{v} \cdot \mathbf{n}) d\Gamma \\ & - \int_{\partial B_\varepsilon} \mathbf{C} \varepsilon(\mathbf{u}_\varepsilon) \varepsilon(\mathbf{u}_\varepsilon) (\mathbf{v} \cdot \mathbf{n}) d\Gamma \end{aligned} \quad (81)$$

Based on the relationship for velocity over the boundary in Eq. (43),

$$\begin{aligned} - \int_{\partial \Omega_\varepsilon} \mathbf{C} \varepsilon(\mathbf{u}_\varepsilon) \varepsilon(\mathbf{u}_\varepsilon) (\mathbf{v} \cdot \mathbf{n}) d\Gamma & = - \int_{\partial B_\varepsilon} \mathbf{C} \varepsilon(\mathbf{u}_\varepsilon) \varepsilon(\mathbf{u}_\varepsilon) d\Gamma \\ & = \int_{\partial B_\varepsilon} \left[(\mathbf{C}^{-1} \sigma)^T \sigma + 2\sigma^2 \varepsilon_{th}(T_\varepsilon) + (\mathbf{C} \varepsilon_{th}(T_\varepsilon))^T \varepsilon_{th}(T_\varepsilon) \right] d\Gamma \end{aligned} \quad (82)$$

By substituting tangential stress (76) in boundary integral (82):

$$\begin{aligned} & \int_0^{2\pi} \left[(\mathbf{C}^{-1} \sigma)^T \sigma + 2\sigma^2 \varepsilon_{th}(T_\varepsilon) + (\mathbf{C} \varepsilon_{th}(T_\varepsilon))^T \varepsilon_{th}(T_\varepsilon) \right] \varepsilon d\gamma \\ & = 2\pi\varepsilon \left[\frac{3}{E} ((\text{tr}(\sigma))^2 - \frac{8}{E} \sigma_1 \sigma_2 + 2\alpha T \text{tr}(\sigma) + \frac{2E\alpha^2 T^2}{1-\nu}) \right] \end{aligned} \quad (83)$$

The last term of Eq. 60:

$$\lambda \int_{\partial\Omega_\varepsilon} \mathbf{v} \cdot \mathbf{n}d\Gamma = \lambda \int_{\partial\Omega} \mathbf{v} \cdot \mathbf{n}d\Gamma + \lambda \int_{\partial B_\varepsilon} \mathbf{v} \cdot \mathbf{n}d\Gamma \tag{84}$$

Based on the relationship for velocity over the boundary in Eq. (43),

$$\lambda \int_{\partial\Omega_\varepsilon} \mathbf{v} \cdot \mathbf{n}d\Gamma = -\lambda \int_{\partial B_\varepsilon} d\Gamma = -2\pi\varepsilon\lambda \tag{85}$$

The surface function of the hole is denoted by $f(\varepsilon)$:

$$f(\varepsilon) = -|B_\varepsilon| = -\pi\varepsilon^2 \Rightarrow f'(\varepsilon) = -2\pi\varepsilon \tag{86}$$

Further, by substituting in the topological derivative (Eq. (48)), the Lagrangian topology function is obtained:

$$D_T L = -\frac{1}{\pi\varepsilon} \left[\alpha T' tr(\sigma) + \frac{2E\alpha^2 T T'}{1-\nu} \right] - \frac{3}{E} ((tr(\sigma))^2) + \frac{8}{E} \sigma_1 \sigma_2 + \frac{2E\alpha^2 T^2}{1-\nu} + \lambda \tag{87}$$

5. Numerical Examples

An optimization problem was tackled for the structure in the figure below (Fig. 3.). First, the analysis was carried out for uniform temperature boundary conditions. Based on the figure, the structure is secured on the left and right by clam supports. The mechanical boundary conditions were defined by a concentrated force ($F = 1 N$) in the middle of the lower edge of the structure. Temperature boundary conditions were distributed on the right and left edges of the structure. The material properties were defined by Young’s modulus $E = 1$, thermal conductivity $k = 1$, thermal expansion coefficient $\alpha = 1 \times 10^{-4}$ and Poisson’s ratio $\nu = 0.3$.

A total of fifty and twenty elements were considered in the horizontal and vertical directions, respectively. The optimization results for the level-set-based method are presented by the compliance objective function and a volume constraint using the reaction diffusion equation under both identical and different temperature boundary conditions.

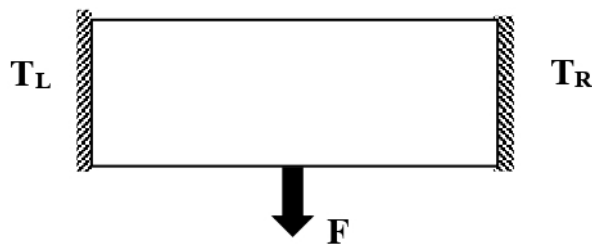


Fig. 3. The initial shape of the structure under temperature and mechanical boundary conditions.

The results were compared with the reports of Xia et al. [39] under identical temperature boundary conditions, with a volume constraint of $\bar{V} = 0.2$. The first row of Figure (4) corresponds to the case with only mechanical boundary condition. The second and third rows of Figure (4) correspond to identical temperature boundary conditions, under which the elements do not exhibit considerable temperature variations during optimization, thus producing identical temperatures across all elements. The results were compared with those reported by Xia for fixed-temperature elements.







$\bar{V} = 0.2$	Proposed method	Xia's work
$T_R = T_L = 0$		
$T_R = T_L = 5$		
$T_R = T_L = 15$		

Fig. 4. A comparison of the final optimized forms in the present study with those of the Xia et al. under identical temperature boundary condition with the volume constraint $\bar{V} = 0.2$.

Figure (5) illustrates temperature variations in element no. 976, located in the middle of the lower edge, during optimization under identical temperature boundary conditions ($T_R = T_L = 5$). As evident, in this topology, the temperature of the elements remains identical and unchanged during the optimization.

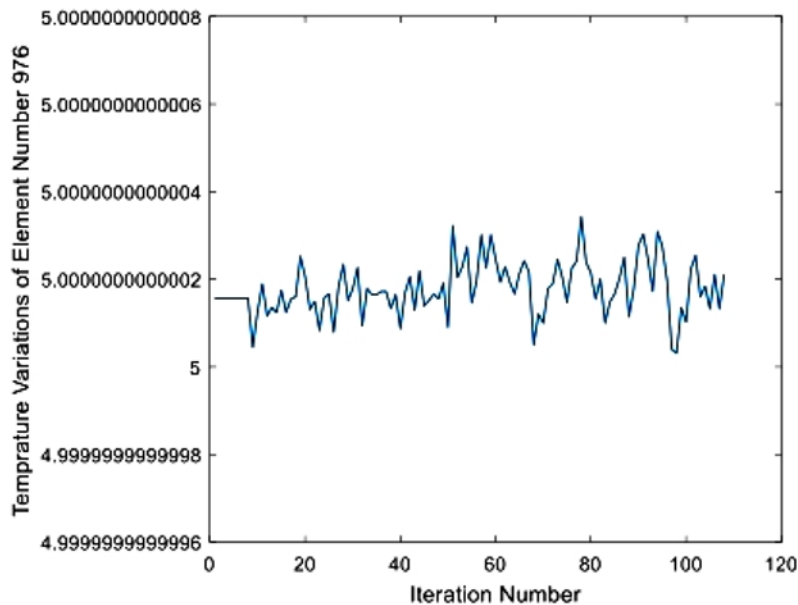


Fig. 5. Temperature variations in element no. 976, located in the middle of the lower edge, during optimization under identical temperature boundary conditions ($T_R = T_L = 5$).

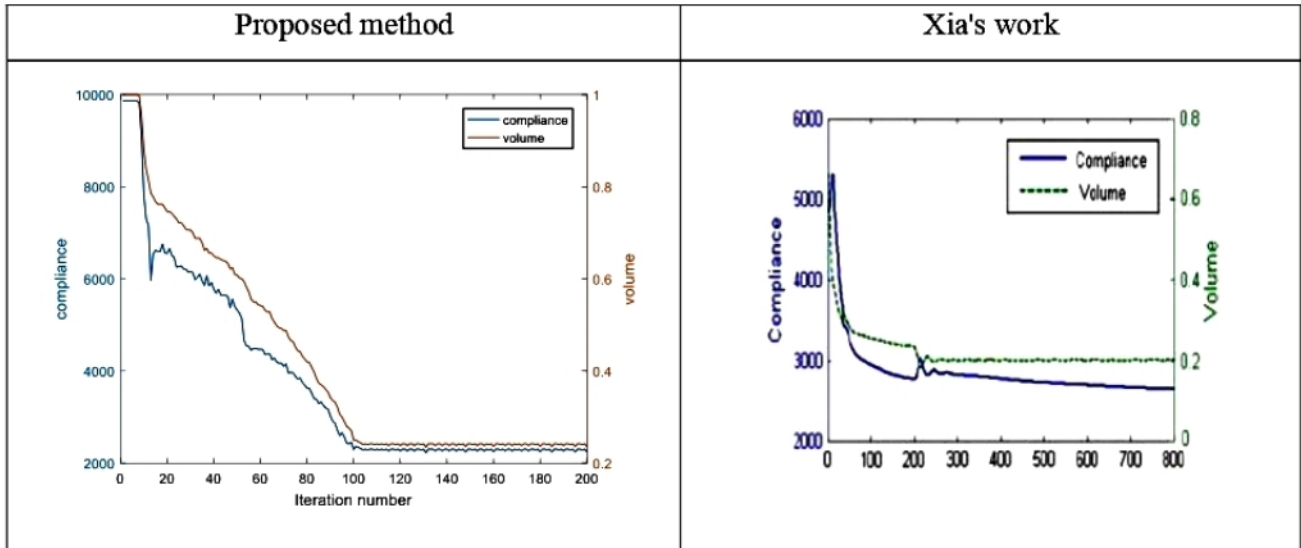


Fig. 6. The comparison of the compliance and volume constraint in the proposed method with Xia’s work at $T_R = T_L = 5$.

As can be seen from Figure (6), the convergence rate in the proposed method is higher than the Xia’s work. Figure (7) compares the results with those from the homogenization method [29] under identical temperature boundary conditions with the volume constraint $\bar{V} = 0.4$.

$\bar{V} = 0.4$	Proposed method	Homogenization method
$T_R = T_L = 0$		
$T_R = T_L = 1$		
$T_R = T_L = 4$		

Fig. 7. A comparison of the final optimized forms in the present study with those from homogenization method under identical temperature boundary condition with the volume constraint $\bar{V} = 0.4$.

The problem is investigated under different temperature boundary conditions. Under non-identical boundary conditions, the temperature, a function of the topology, changes in the elements throughout the optimization. As a result of the decrease in the number of elements in the topology, in addition to elasticity modulus, a penalty is applied to the thermal conductivity of the elements. Therefore,

the temperature changes in the elements in every optimization step. Optimization under different temperature boundary conditions is presented in four cases, according to Figure (8).





$\bar{V} = 0.5$	Proposed method
$T_R = 1$ $T_L = 5$	
$T_R = 5$ $T_L = 1$	
$T_R = 15$ $T_L = 5$	
$T_R = 5$ $T_L = 15$	

Fig. 8. The final optimized forms by the proposed method under non-identical temperature boundary condition with the volume constraint $\bar{V} = 0.5$.

Figure (9) illustrates temperature variations in element 976, located in the middle of the lower edge, during optimization under the third-case temperature boundary conditions ($T_R = 15$ and $T_L = 5$).

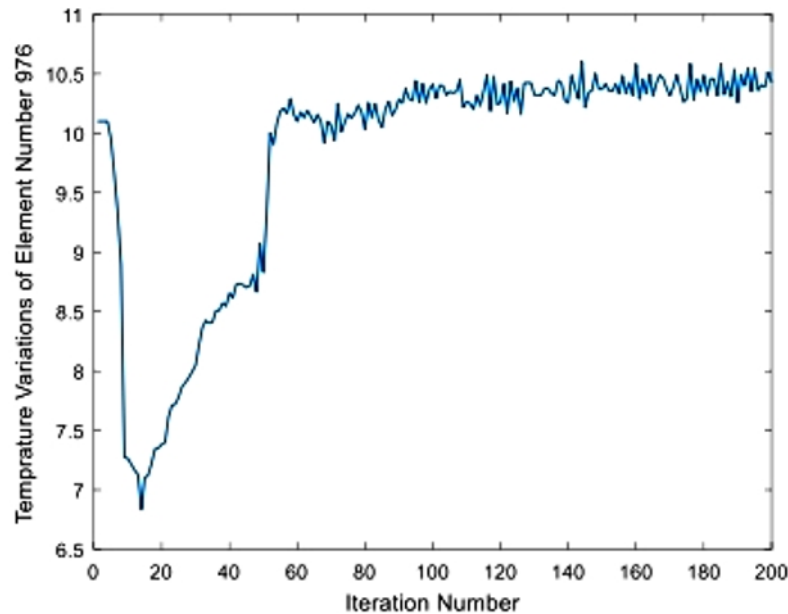


Fig. 9. Temperature variations in element no. 976, located in the middle of the lower edge, during optimization under non- identical temperature boundary conditions ($T_R = 15$ and $T_L = 5$).

6. Conclusion

In this work, we have derived new term in reaction diffusion equation for considering the effects of temperature boundary conditions. Applying this new formulation, the topology function derived for temperature and mechanical boundary conditions, the topology optimization is analyzed in two modes. In the first case with identical temperature boundary conditions, the results show that penalizing the thermal conductivity of eliminated elements has no significant effects on the temperature of remaining elements during optimization. In this case, the results obtained from the proposed method are consistent with those obtained by Xia's work and homogenization method. In the second mode with non-identical temperature boundary conditions, topological variations significantly affected the temperature of remaining elements during optimization. In fact, penalizing the thermal conductivity of eliminated elements causing variations in the conductivity matrix and thereby temperature of elements.

References

- [1] G. Allaire, F. De Gournay, F. Jouve, AM. Toader, Structural optimization using topological and shape sensitivity via a level set method, *Control. Cybern.* 34(1) (2005) 59-80.
- [2] G. Allaire, F. Jouve, A.M. Toader, Structural Optimization Using Sensitivity Analysis and a Level Set Method, *Journal of Computational Physics.*194 (2004) 363-393.
- [3] S. Amstutz, A. Novotny, Topological optimization of structures subject to Von Mises stress constraints, *Struct. Multidiscip. Optim.* 41 (2010)407-420.
- [4] M.P. Bendsoe, N. Kikuchi, Generating optimal topologies in structural design using a homogenization method, *Comput. Methods Appl. Mech. Engrg.* 71 (1988) 197-224.
- [5] M.P. Bendsoe, Optimal shape design as a material distribution problem, *Struct. Optim.* 1 (1989) 193-202.
- [6] MP. Bendsoe, O. Sigmund, Material interpolation schemes in topology optimization, *Arch. Appl. Mech.* 69(9-10) (1999) 635-654.
- [7] MP. Bendsoe, O. Sigmund, *Topology optimization: theory, methods and applications.* Springer. Berlin. (2003).
- [8] M. Burger, B. Hackl, W. Ring, Incorporating topological derivatives into level set methods, *J. Comput. Phys.* 194(1) (2004) 344-362.
- [9] J. Cea, S. Garreau, P. Guillaume, M. Masmoudi, The shape and topological optimizations Connection, *Comput. Methods. Appl. Mech. Eng.* 188(4) (2000) 713-726.

- [10] K.K. Choi, N.H. Kim, *Structural Sensitivity Analysis and Optimization*, Springer, 2005.
- [11] H. Chung, O. Amir, H. A. Kim, Level-set topology optimization considering nonlinear thermoelasticity, *Comput. Methods Appl. Mech. Engrg.* (2019).
- [12] J. Deaton, R. V. Grandhi, Topology Optimization of Thermal Structures with Stress Constraints, presented at the 54th AIAA/ASME/ASCE/ASC Structures, Structural Dynamics, and Materials Conference, Boston, MA, (2013).
- [13] S. Deng, K. Suresh, J. Joo, Stress-Constrained Thermo-Elastic Topology Optimization: A Topological Sensitivity Approach, presented at the Proceedings of the ASME IDETC/CIE Conference, Buffalo, NY, USA, (2014).
- [14] H.A. Eschenauer, H.A. Kobelev, A. Schumacher, Bubble Method for Topology and Shape Optimization of Structures, *Struct. Multidisc. Optim.* 8 (1994) 42-51.
- [15] R. Feijoo, A. Novotny, E. Taroco, C. Padra, The topological-shape sensitivity method in two-dimensional linear elasticity topology design, in: *Applications of Computational Mechanics in Structures and Fluids*, 2005.
- [16] R.A. Feijoo, A.A. Novotny, E. Taroco, C. Padra, The topological shape sensitivity method in two-dimensional linear elasticity topology design, *J. Comput. Methods Sci. Eng.* (2005).
- [17] T. Gao and W. Zhang, Topology optimization involving thermo-elastic stress loads, *Struct. Multidiscip. Optim.* 42 (2010) 725-738.
- [18] S. Garreau, P. Guillaume, M. Masmoudi, The topological asymptotic for PDE systems: the elasticity case, *SIAM. J. Control. Optim.* 39 (2001) 1756.
- [19] L. Li, H. A. Kim, Multiscale Topology Optimization of Thermoelastic Structures using Level Set Method, *American Institute of Aeronautics and Astronautics*, (2020).
- [20] D. Li, X. Zhang, Topology Optimization of Thermo-Mechanical Continuum Structure, presented at the 2010 IEEE/ASME International Conference on Advanced Intelligent Mechatronics, Canada, (2010).
- [21] X. Liu, C. Wang, Y. Zhou, Topology optimization of thermoelastic structures using the guide-weight method, *Sci. China Technol. Sci.* 57(5) (2014) 968-979.
- [22] D. J. Neiferd, R. V. Grandhi, Level-set Topology Optimization of Thermoelastic Structures - A Comparison of Compliance, Strain Energy, and Stress Objectives, *American Institute of Aeronautics and Astronautics*, (2018).
- [23] J. Nocedal, S.J. Wright, *Numerical optimization*, Springer, (1999).
- [24] A.A. Novotny, R.A. Feijoo, E. Taroco, C. Padra, Topological sensitivity analysis, *Comput. Methods Appl. Mech. Engrg.* 192 (2003) 803-829.
- [25] A. Novotny, R. Feijoo, E. Taroco, C. Padra, Topological sensitivity analysis for three-dimensional linear elasticity problem, *Comput. Methods Appl. Mech. Engrg.* 196 (2007) 4354-4364.
- [26] J. S. Osher, F. Santosa, Level Set Methods for Optimization Problems Involving Geometry and Constraints: I. Frequencies of a Two-Density Inhomogeneous Drum, *J. Comput. Phys.* 171(1) (2001) 272-288.
- [27] M. Otomori, T. Yamada, K. Izui, S. Nishiwaki, Matlab code for a level set-based topology optimization method using a reaction diffusion equation, *Struct. Multidisc. Optim.* 2014.
- [28] D. Reynolds, J.P. McConnachie, W. Bettess, C. Christie, J.W. Bull, Reverse Adaptivity - a New Evolutionary Tool for Structural Optimization, *Int. J. Numer. Methods Eng.* 45 (1999) 529-552.
- [29] H. Rodrigues, P. Fernandes, A material based model for topology optimization of thermo-elastic Structures, *International Journal for Numerical Methods in Engineering*, 38 (1995) 1951-1965.
- [30] A. Schumacher, *Topologieoptimierung von bauteilstrukturen unter verwendung von Lopchpositionierungskriterien*, PhD thesis. Universit at-Gesamthochschule Siegen. Siegen. Germany. 1995.
- [31] J.A. Sethian, A. Wiegmann, Structural Boundary Design via Level Set and Immersed Interface Methods, *J. Comput. Phys.* 163(2) (2000) 489-528.
- [32] J. Sokolowski, A. Zochowski, On the Topological Derivative in Shape Optimization, *SIAM Journal of Control Optimization.* 37 (1999) 1251-1272.
- [33] M. Stolpe, K. Svanberg, An alternative interpolation scheme for minimum compliance topology optimization, *Struct. Multidiscip. Optim.* 22 (2001) 116-124.
- [34] N. Vermaak, G. Michailidis, G. Parry, R. Estevez, G. Allaire, Y. Bréchet, Material interface effects on the topology optimization of multi-phase structures using a level set method, *Struct. Multidiscip. Optim.* (2014) 1-22.
- [35] X. Wang, MY. Wang, D. Guo, Structural shape and topology optimization in a level-set-based framework of region representation, *Struct. Multidisc. Optim.* 27(1) (2004) 1-19.
- [36] MY. Wang, S. Chen, X. Wang, Y. Mei, Design of multimaterial compliant mechanisms using level-set methods, *J. Mech. Des.* 127 (2005) 941-956.
- [37] M.Y. Wang, X.M. Wang, D.M. Guo, A Level Set Method for Structural Topology Optimization, *Comput. Methods Appl. Mech. Eng.* 192 (2003) 227-246.
- [38] M.Y. Wang, X.M. Wang, 'Color' Level Sets: a Multiphase Method for Structural Topology Optimization with Multiple Materials, *Comput. Meth. Appl. Mech. Eng.* 193 (2004) 469-496.

- [39] Q. Xia, M.Y. Wang, Topology optimization of thermo-elastic structures using level set method, *Comput. Mech.* 42 (2008) 837-857.
- [40] Y.M. Xie, G.P. Steven, A Simple Evolutionary Procedure for Structural Optimization, *Comput. Struct.* 5(1993) 885-896.
- [41] Y.M. Xie, G.P. Steven, *Evolutionary Structural Optimization*, Springer-Verlag London Limited. UK. 1997.
- [42] Xing and Xianghua, A Finite Element Based Level Set Method for Structural Topology Optimization, PHD thesis. 2009.
- [43] T. Yamada, K. Izui, S. Nishiwaki, A. Takezawa, A topology optimization method based on the level set method incorporating a fictitious interface energy, *Comput. Methods Appl. Mech. Eng.* 199 (2010) 2876-2891.
- [44] X. Yang, Y. Li, Topology optimization to minimize the dynamic compliance of a bi-material plate in a thermal environment, *Struct. Multidiscip. Optim.* 47 (2012) 399-408.
- [45] X. Yang, Y. Li, Structural topology optimization on dynamic compliance at resonance frequency in thermal environments, *Struct. Multidiscip. Optim.* 49 (2013) 81-91.
- [46] M. Yulin, WA. Xiaoming, level set method for structural topology optimization and its Applications, *Adv. Eng. Softw.* 35(7) (2004a) 415- 441.
- [47] W. Zhang, J. Yang, Y. Xu, T. Gao, Topology optimization of thermoelastic structures: mean compliance minimization or elastic strain energy minimization, *Struct. Multidiscip. Optim.* 49(3) (2013) 417-429.